ELSEVIER

Thermochimica Acta 310 (1998) 1–17

thermochimica acta

Sub-micrometer thermal physics – An overview on SThM techniques[1]

E. Gmelin*, R. Fischer, R. Stitzinger

Max-Planck-Institut für Festkörperforschung, D-70569 Stuttgart, Heisenbergstraße 1, Germany

Received 14 May 1997; accepted 16 June 1997

Abstract

The historical development and present state of the art of scanning thermal microscopy (SThM) – temperature profiling, thermography and other measurements of thermal parameters – in the sub-μm range and the relevant thermal sensors are reviewed. The paper proposes a classification scheme for the various experimental arrangements of STM and AFM based SThM's. Limitations of the SThM technique and future prospects are briefly discussed. © 1998 Elsevier Science B.V.

Keywords: Thermal instruments; Scanning probe microscopy: components and technique; Thermometry: 7.20-n, 7.79-v, 7.20.DT

1. Introduction

The steady and increasing trend towards miniaturization of micro-electronic and micro-mechanical devices into the sub-micrometer scale has led into enhanced research activities for very different physical and chemical parameters in the mesoscopic range. Progress of science and engineering in the mesoscopic range was revolutionized by the invention of the scanning tunneling microscope (STM) and atomic force microscope (AFM) [1] followed by a rapid and manyfold development in the field of experimental scanning-probe-techniques [2]. These instruments and their numerous modifications, e.g. thermal [3], friction [4], magnetic [5], electrostatic [6] and capacitive [7] microscopes, opened new frontiers in research on ultra-small scales of the involved physical quantities, i.e. space, energy, time and temperature. Similarly, this technique significantly promoted the instrumental development in other areas, in particular, it initiated a wealth of optical methods for the determination of temperature profiles in microstructures [9]. These tools bear an enormous potential of practical application, e.g. single atomic switching, submicrometer temperature profiling, (local) energy measurement in the nano- or femto Joule range, or even lower. Most desirable is the simultaneous profiling of topographical and thermal structures of the material studied.

Looking today on the wide-spread and various activities in the context of STM and AFM equipment and experiments, three features are remarkable: (i) the application of STM and AFM, worked out by physicists, remained restricted essentially to physical phenomena, the use for the investigation of chemical processes is just starting, (ii) in contrast to numerous studies on the structural and electronic properties of

*Corresponding author. Fax: 0049-711/689 1010; e-mail: gmelin@tilux.mpi-stuttgart.mpg.de

[1]Presented at the Twelfth Ulm-Freiberg Conference, Freiberg, Germany, 19–21 March 1997

PII S0040-6031(97)00379-1

materials, thermal measurements have been performed rather scarcely, only recently progress can be noted when the feasibility of STM and AFM technology for the characterization of thermal material properties and thermal imaging has been demonstrated, (iii) there is a rapidly increasing number of different experimental arrangements (for STM and AFM) and sensor technology reported in the literature that becomes difficult to overlook. It is for these reasons that we decided to write this contribution where we review the basic instrumental developments, try to classify the reported setup's, make a collection of the presently available sensors and intend to outline for which purpose micro-thermophysical research may serve and to which extend it can be done. We address with preference to non-experts in this new and exciting field of science which displays the potential to radiate to many other disciplines of engineering and research. We note that optical methods as well as the very new and attractive near-field thermometric devices have been deliberately excluded from this overview.

In the first part of this paper (Section 2), we summarize the academic and practical motivation for thermal experiments in the sub-micrometer range and try to point out its limitations. Second, we outline briefly the historical development, present the state of the art by describing the methods applied and propose a classification for the scanning thermal microscope equipment. The fourth and fifth section is devoted to sensors and thermography, applications and limitations of this technology.

2. Mesoscopic thermo-physics: motivations, applications and limitations

How to define micro-thermophysics? Novel phenomena arise when the geometrical dimensions (characterized by a length d) reach critical values [8,9]. Electronic and thermal transport in solids are strongly afflicted by reduction of the sample geometry towards dimensions comparable to the mean free path 1_f of the carriers and the phonons ($d \leq 1_f$). Under such conditions, size-effect phenomena [8,10], effects of mean free paths of quasi-particles [11], ballistic carrier transport [12], asymmetric heat production [13], electron–phonon interaction [14,15] and its suppression [16,17] ('phonon-drag quenching') may occur. Quantum effects appear when the confinement dimensions are of the order of a few nanometers such as seen in quantum wells of compound semiconductors [18,19]. The fundamental quantities involved in thermophysical measurements are temperature T and temperature differences ΔT, energy E and energy changes ΔE, heat Q and heat flow Φ, and the corresponding quantities derived, e.g. thermoelectric power S. There exists an intimate relation between the length scale and the thermal quantities: extensive thermodynamic parameters are extremely reduced when approaching atomic scale, intensive parameters may change significantly or may even become undefined. Thus, mesoscopic ($d \approx 1_f$) or ballistic ($d \ll 1_f$) experimental conditions seriously affect the thermal quantities describing the quasi-particle transport properties, i.e. when the measurement is performed within the length (or volume) scale, $d < 1_f$, or a time scale much shorter than that required to establish thermal equilibrium. In the extreme limits, the Boltzman equation may loose its validity and irreversible thermodynamics must be applied [20].

What is the motivation to develop instrumentation for the detection of thermal quantities with the highest possible spacial (nm-range), energetical (fJ-range), and temporal (ns/ps-range) resolution?

There are two issues involved, (i) a practical one, i.e. the necessity to solve a number of important application-oriented problems, and (ii) an academic interest that intends to understand both, fundamental and new problems.

Spatially high-resolution determination of temperature and temperature distribution, heat flow measurement and detection of local power dissipation in the sub-μm range have become fundamental for microelectronics. Highly integrated microelectronic devices, with preference to high power chips but also optoelectronic systems, e.g. quantum-well lasers, evolve many problems because uncontrolled heat dissipation reduce their performance and lifetime, or even destroy them. Semiconductor devices must withstand short-time electrical stressing phenomena which may induce severe degradation or total failure due to uncontrolled temperature effects (thermomigration, overheating even melting). The knowledge of the microscopic thermal behaviour, displayed by locally and temporally highly resolved temperature

measurements may avoid electronic device failure, improve their performance, give indication on thermal boundary resistance and thus remove 'hot spots'. Any dissipation of heat or change of energy, e.g. radiative or non-radiative recombinations of holes or electrons, photoeffect, etc., can presumably be studied soon by thermo-tips. Simulation of such thermal failure phenomena needs experimental transient temperature field data for the verification of the modelling parameters used. Similarly, the impact of nanometer-scale heat transfer on designing and engineering of micromechanical systems, e.g. flow actuators, micropumps, etc., and in artificial nanostructures, e.g. two- and three-dimensional nano-pores, nano-tubes and nano-wires, as well as in biological membranes, may become significant for sensoric and catalysis application purpose. Their performance or failure can be thermally optimized or avoided, respectively. The development of small-sized, highly sensitive reactive sensors for gases and liquids, for environmental science and for thermoanalytical micro-instrumentation equally falls under this topic [21,22]. For material sciences, the local determination of the steady state and transient temperature fields, of the heat conductivity and its local anisotropy and of the heat capacity of microscopic structures constitutes a basic tool to understand, to model and to design microscopic structures such as semiconductor devices, thin films, interconnects and interfaces, powdered materials, whiskers, multi-layer and compound materials, grain boundaries, intergranular phases, coatings, the behaviour of thermal lenses, etc. Such investigations are not possible with the classical experimental equipment.

Basic researchers expect to get more insight into the overall problems of heat transfer and in mesoscopic systems and in the problems like electron–phonon interaction, ballistic heat transport, heat flow in low dimensional/geometrically restricted solids, near-field effects, e.g. processes which govern the contactless measurement of temperature in vacuum in the nm-range, local determination of electrochemical potentials, chemical reaction under geometrical restriction (as outlined before), and finally to make out the limits of classical heat transport formalism (Boltzman equation). In this context, for example, the understanding of contactless heat transport in vacuum, not mediated by radiative heat, remains an open question. Some mechanisms have been proposed; these are listed in Table 1. None of them has been verified or confirmed experimentally.

The use of the STM and AFM technologies makes it possible to research the nano-meter range. However, not every type of experiment may be meaningful: for thermal measurements the limitations are more stringent than for topographical or energetical experiments. Thermal experiments are described by Boltzmann's equation based on thermal equilibrium. This equilibrium, and therewith the definition of temperature-difference and/or heat transferred becomes questionable as soon as the mean free paths of the relevant quasi-particles become larger than the geometrical sizes involved. On the other hand, energy can always be transferred, e.g. from one atom to the other. Important questions remain unexplored yet, e.g. whether quantization of heat-flow can be detected by this way or to what extend the nanometer-scale experiments (chemical reaction, gas detection on an AFM tip) can be extrapolated to 'large' scale processes, e.g. chemical process engineering. For the latter, it seems that the limits are reached quickly and lay in the mm-range. In addition, mechanical stability of the sample, e.g. thin films, and the increased influence of surface, surface-defects, defects

Table 1
Mechanisms of heat transfer for point-contacts (e.g. thermo-tip) and the relevant distance dependence, estimated for a micro-thermocouple with a heat capacity between 2.10^{-2} fJ/K and 3 pJ/K [26]

Mechanism	Transferred energy E (pW)	Functional dependence on distance d
Heat conductivity, ballistic	7.10^{-6}	None
Heat conduction by gas (NPT)	2.10^{-2}	None
Heat radiation, classical	6.10^{-4}	None
Heat transfer, near-field	–	$\sim d^{-4}$
Tunneling effect	1.10^{-2}	$e^{-2\mathrm{kd}}$
Pressure effect	–	$\sim U^{1/3}$

in general and their spacial distribution can hinder or prevent meaningful results. The calibration of the micro-sensors used in STM or AFM, with respect to temperature and/or energy, is problematic.

The field of 'thermal' STM and AFM is new and develops rapidly. Therefore, a comprehensive review doesn't exist, however, some of the recent publications presented the essential features of the different technologies; we refer to Refs. [3,23–27]. Presently, the largest advance occurs in simultaneous topographic and thermal probing of sample surfaces, the so-called thermography in which structural–topographic analysis (by STM or AFM) is combined with mapping the temperature of the same structure.

3. Historical and technological development and state of the art

The STM/AFM technology is best suited to study thermal phenomena in the sub-mm scales. The instrument then is denoted as scanning thermal microscope (SThM) which is based either on the STM or AFM construction principle. Before giving in short a description of the historical events and recent technological achievements, we discuss the present and possible future resolution of SThM's, describe schematically the basic methods developed for SThM and try to establish a classification of the numerous modifications of STM and AFM's, working as SThM, which have been reported in the literature.

3.1. The resolution in temperature, space and time

In view of resolution, 'mechanical and electrical' measuring techniques are much better developed than thermal instrumentation. Single atoms size (spatial resolution 1 Å) and charge (resolution 10^{-19} Cb) can be detected with STM and AFM whereas the resolutions achieved in temperature and energy measurements (as well as heat/heat-flow experiments) remain far below their limits of resolution; this is in principle kT which is at room temperature about 10^{-21} J. The temperature, however, is the basic experimental quantity measured from which the other thermal quantities (Q, Φ, and ΔE) are mostly derived.

Temperature is monitored with a large number of different methods and sensors [28], either resistively with metallic or semiconducting resistors [29], semiconductor diodes or thermistors [28], or thermoelectrically by thermocouples [30], or optically by surface reflectance [31], infrared thermometry or Raman spectroscopy [32], fluorescence imaging [33], photothermally (thermally-induced surface displacement) [34,35], photoacoustically or thermoelastically [36]. The wealth of optical methods have been developed in the eighties and nineties for the determination of steady state and transient temperature, heat conductivity and capacity, e.g. the laser-flash method, the 'mirage' effect, thermal modulation techniques and the afore-cited photo-thermal and photo-acoustic methods. The most recent research developed elaborated near-field optical techniques to register temperature profiles in the sub-μm and sub-μs ranges as well as mapping of temperature fields in semiconductor devices [29,37,38] using, e.g. high resolution laser-reflectance thermometry [38,39], The spatial resolution has been extended to 50 nm and the temporal one to 10 ns, respectively. Each of these methods and each type of thermometric technique applied displays its own advantages with respect to spatial, temporal and temperature resolution. Some of the techniques are listed in Table 2. In the context of STM and AFM, thermoelectric and resistive sensors play a role: very small thermocouple-tips or ultra-fine electrical wires (as resistance thermometer) serve as temperature detectors. Although recently modern nanofabrication technology was applied to produce sub-nanometer thermal tips, however, their sensitivity and resolution does not go beyond that what is known for the relevant classical thermometer materials. Moreover, thermoelectricity of known bulk materials, Si or AuFe, drops drastically when measured in a geometrically restricted arrangement [16,17], e.g. as being present in an AFM tip, presumably due to dimensionality effects ('phonon-drag quenching', surface defects, inhomogeniety).

The highest temperature resolution results from resistance or quartz resonant thermometry, resolving μK or better. The spatial resolution of a thermometer is given by its geometrical size. The highest spatial resolution guarantees application of the STM/AFM technique. The fastest temporal resolution is achieved with all the optical (spectroscopic) methods which enable to measure below the μs-range. Optical and photothermal techniques yield also excellent spatial

Table 2
Temperature, spatial and temporal resolutions achieved using different experimental methods

Technique	Resolutions achieved for:		
	Temperature T (K)	Local x (μm)	Time t (ms)
Thermocouple	0.01	10	1
Semiconductor diode	0.001	10	0.01
Metallic resistor	0.01	20	0.005
Thermistor	0.001	50	5
Infrared thermometry	1	30	–
Near-field thermometry	0.05	0.01	<0.0001
Surface reflectance	0.01	0.5	0.0001
Raman spectroscopy	1	0.5	2
Liquid-crystals	0.5	80	>1
Magnetic resonance	1	300	–
Quartz resonator	0.00001	>10	<0.01
Photothermal	0.01	10	0.1

resolution and resolve down to 100 nm. The diffraction of the wavelength of the light used limits the far-field optical technique but not when near-field optics is used. Scaling down the size of a thermometric sensor correspondingly, reduces its heat capacity and therefore shortens the thermal relaxation time. A thermoelectric tip of 0.25 mm diameter and conically formed with an angle of 20 degree enables one to achieve a very short thermal response time [26]; values as low as 100 ns have been reached [34]. The application of the modern nanofabrication technologies offers the possibility to provide thermocouple sensors of the size of 100 nm or below.

3.2. Scanning thermal microscopy (SThM) – methods and classification

The principle of SThM's based on the STM or AFM technology is schematically shown in Fig. 1 and 2. The key element of the STM based thermal microscope (Fig. 1) is the ultra small thermal probe (thermo-tip) which provides the sensitivity and the spatial resolution necessary to achieve high resolution temperature mapping. The sample (or probe) is usually placed on a laterally and vertically movable piezoelectric drive system (denoted by XYZ in Fig. 1). In the classical STM technique, the topographical map of the sample-surface results from the servo-loop between a metallic tip and the piezo-drive that holds constant the electronic tunneling current, i.e. the distance, between tip and sample by actuating

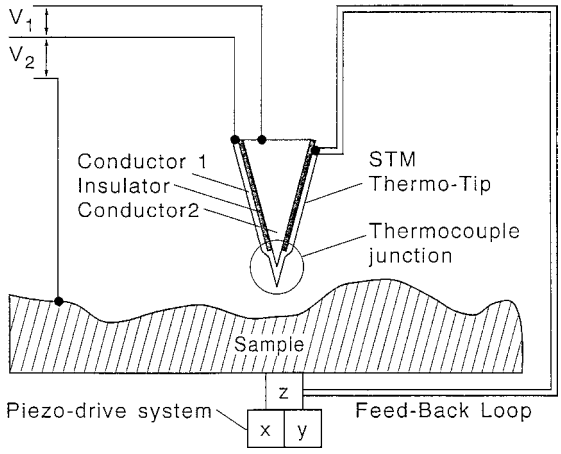

Fig. 1. Schematic arrangement of an STM (scanning tunneling microscope) based Scanning Thermal Microscope (SThM). The thermo-tip (thermocouple junction) scans the temperature profile of the sample. The three-directional movement is controlled by the piezoelectric drive.

the corresponding vertical (Z-directional) piezo-drive while scanning the surface. In the first SThM reported, Williams and Wickramasinghe [3,41,42] and Dransfeld and Xu [43] replaced the conventional metallic tip by a thermocouple sensor produced at the tip apex by the junction of the dissimilar inner and outer conductors 1 and 2 (Fig. 1) separated by an insulator. The thermocouple (operated by the standard technique of keeping another reference-junction at a constant temperature) generates a temperature-dependent voltage V_1 which provides the means for remotely sensing the

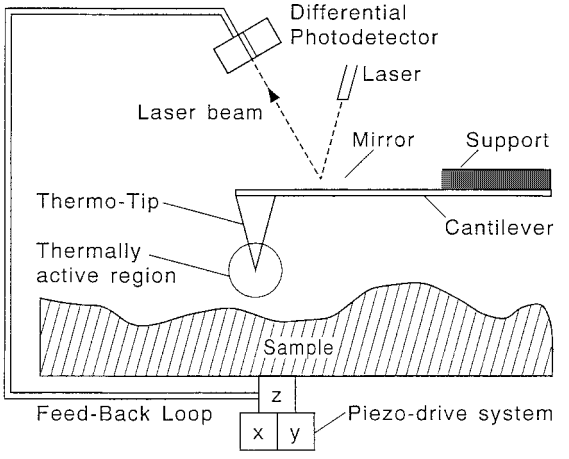

Fig. 2. Schematic arrangement of an AFM (atomic force microscope) based Scanning Thermal Microscope (SThM). The deflection of the cantilever and tip ensemble is here detected by a difference photodetector via a laser beam.

local tip temperature when it is scanned laterally across the surface. In contrast to classical STM, however, the feed-back-loop adjusts the vertical tip position of the probe, i.e. the distance between probe and sample to maintain a constant thermal flux between probe and sample, rather than a constant tunneling current. This working mode does not give a thermal but a topological image of the surface [41,42]. For temperature mapping, either the sample or the tip is heated. If the temperature variation resulting from, e.g. heating of the sample, is small compared to the temperature difference between probe and sample, then simultaneous and independent images of the surface topography and temperature can be obtained. The probe is often vibrated vertically at a frequency ω_1 (to avoid problems with temperature variation or thermal noise) whereas the sample temperature is modulated at a frequency ω_2, where ω_1 (feed-back-loop) is outside the bandwidth of ω_2 [42].

The general disadvantage of the described STM arrangement consists in the requirement of electrically conducting surfaces for the experiment when simultaneously topography and temperature profiles are to be measured. The tunneling current is needed to control the gap distance (sample-to-tip) whereas the thermovoltage monitored maps the temperature.

SThM's based on the AFM principle avoid this disadvantage. Therefore, the AFM system finds preferentially application as SThM: (i) electrically conducting and non-conducting (isolating) surfaces can be scanned thermally, and (ii) the force feed-back control system does not interfere with the operational principle of many sensors. Fig. 2 displays a schematic diagram of an AFM-based SThM set-up. Again, likewise to the STM based SThM, a thermometric sensor replaces the metallic tip of the classical AFM. The AFM consists of a sharp tip mounted on a cantilever which is brought close to the sample surface by the piezoelectric actuators acting either on the sample or the tip probe. The deflection of the cantilever due to probe-to-sample interatomic forces are for example optically detected by reflecting a laser beam from a mirror placed on the cantilever towards a differential photo-detector (Fig. 2). The spring constant of the cantilever determines the magnitude of the optical deflection resulting from the tip-to-sample force (10–20 nN) bending the cantilever. The elastic properties of the cantilever can be adjusted to obtain the desired spring constant. While the feed-back loop maintains a constant force by actuating the piezo-drive system, the tip scans over the sample surface and produces a topographical image with nearly atomic resolution. Replacing the tip by any tip-thermometer, e.g. a thermocouple junction as described above, the probe allows for simultaneous mapping of the topography and temperature profile of the sample surface. It is obvious that with the AFM based set-up the tip positioning is independent of the thermal signal management since the feed-back mechanism is force-based whereas the thermal signal originates from a 'different' device.

The heart of any SThH is the microthermal sensor (tip, probe) and, in contrast to STM and AFM, the presence of a temperature differences, either on the sample surface or between sample and thermal probe is needed whereas in conventional STM/AFM experiments temperature differences must be avoided. Three main types have been developed in the recent years: Thermocouple junction, electrical resistance and bimetallic strip. These sensor are schematically shown in Fig. 3, a resistive wire-tip, a micro-thermocouple and a bimetal.

The thermocouple probe (Fig. 3(b)) is made from various dissimilar conductors, e.g. starting with a conical Pt/Ir or W tip (conductor 2 in Fig. 1) identical to those usually taken for STM experiments. Proces-

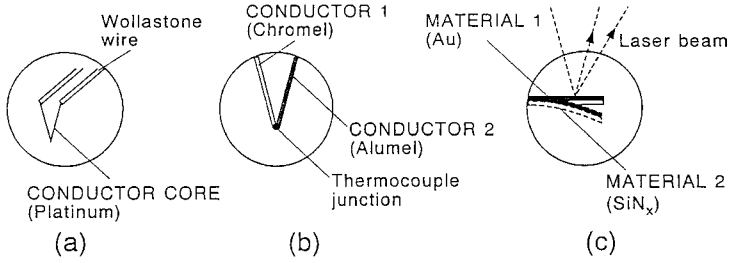

Fig. 3. Schematic diagrams of the various thermo-sensors used in SThM: (a) Resistive probe made from a Wollastone process wire, (b) Thermocouple junctions made from two dissimilar materials (conductor 1 and 2), (c) Bimetallic sensor.

sing of this tip, to fabricate a thermo-sensor, is as follows: first, it is covered with an insulation (thickness about 0.1–10 μm) in a way that a very small length (few μm) at the lower end and a small part (2 mm) at the rear end remain free; then a second metallic component (conductor 1), is sputtered on the tip, except for the rear end. Here we selected an Au-0.07% Fe film of thickness ca. 200 nm [26]. This forms the thermoelectric junction on the tip end with an active volume of ca. 10^{-7} mm^3 (tip radius ca. 50 nm). The rears of the two conductors, embedded in the tip-holder, connect to Cu wires and thus form the thermoelectric loop with an appropriate reference thermoelectric junction (for more details see Ref. [26]). Fig. 4(a) depicts the effective thermopower and its temperature dependence for such a Pt (or W) vs. Au-0.07% Fe thermo-tip. The use of semiconductors enables one to achieve significantly higher thermo-voltages and therefore higher thermoelectric sensitivities. Fig. 4(a) also shows an example of a micro thermocouple made of Si vs. Au [40]. The core constitutes of a conical Si-tip with a tip radius of approximately ~0.5 μm. SiO_2 serves as insulator. The second component (conductor 2) is made of Au. The following section gives the description of further thermo-tips as reported in the literature. In some experiments the thermocouple tip is heated by focusing a laser beam on the tip in order to create a temperature difference (heat flux) between sample and tip [44,45].

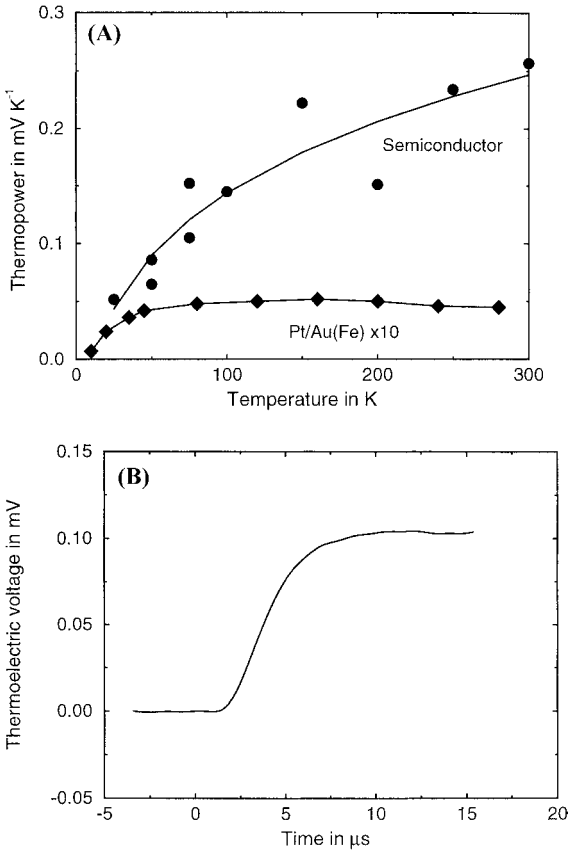

Fig. 4. (a) Seebeck coefficient of micro-thermocouples as a function of temperature: upper curve: Semiconductor (Si, doped $n \approx 10^{19}$ cm^{-3}) vs. Au [40]. lower curve: Pt vs. Au/0.07% Fe [26]. (b) Thermal relaxation curve of the Si vs. Au sensor shown in Fig. 4(a).

Resistive thermal probes, with a sufficiently large temperature coefficient of resistance, are an alternative detector-type that can be well integrated onto the cantilever construction of an AFM [23,46]. The probe is operated in a constant force mode using an AFM and its temperature is monitored by measuring the resistance of the probe (Fig. 3(a)). An advantage of the resistive probe is that it can intrinsically be operated at an elevated temperature, e.g. 40°C, by joule-heating

and so facilitates to generate a temperature difference between the sample studied and the thermo-tip. The relevant tip resistance, respectively temperature is determined by standard bridge technique: the resistive element of the probe makes one of the legs of the bridge feedback circuit, e.g. see Ref. [23]. Currently such probes are fashioned from Wollastone process wire which typically consists of a thin Pt core (ca. 5 μm diameter) surrounded by a thick silver tube (ca. 75 μm diameter). A loop of Wollastone processed wire is formed and attached to the cantilever as schematically shown in Fig. 2. Once the wire is positioned in the AFM, the silver at the end is dissolved on a length of about 200 μm. The thermal sensitivity of a Pt-based resistive thermo-tip amounts to better than 0.1 K.

Finally, micromechanical sensors were recently used, in particular to investigate the heat evolution in chemical reactions [47–52]. As an example, Fig. 3(c) shows schematically a bimetallic sensor which forms the cantilever-tip assembly in an AFM [48]: A 'V'-shaped SiN_3 cantilever with a gold layer (ca. 50 nm thickness) forms the bimetallic strip. A (second) laser spot (50 nm diameter), or an additional resistive heater, focuses on the strip to create a temperature difference with respect to the sample. Temperature changes induce a mechanical vertical deformation (see Fig. 3(c)) of the bimetallic cantilever and a corresponding deflection of the sensing laser beam. Such devices are theoretically able to detect heat changes with atto-Joule resolution. As yet noticed, a large number of different modifications and working modes of SThM set-up's have been reported, which serve as local probes for various surface properties, e.g. temperature profiling [26], thermal imaging [23–25,27,45,53–57], determination of electrochemical potential [58], potentiometric experiments, e.g. to measure the potential along a pn-junction [59,60], contact potentials [61,62], heat conductivity measurements [63], temperature-dependent heat capacity [46], optical absorption [64] a.o. The experiments require particular arrangements and running modes of the SThM.

Hence, it appears useful to classify the various arrangements implemented which will be shortly described in the following. However, at present not all possible combinations have been used. A classification, as listed in Table 3, divides the set-ups according to:

1. principle method used – STM or AFM based,
2. type of thermal sensor applied, electrical or mechanical – thermocouple junction, resistor, pn-junction or bimetal,
3. characteristic working modes (three) – the thermal sensing mode, the heating mode and the mode of the feed-back-loop, and finally according to experimental working conditions.

Table 3 displays that both methods, STM and AFM, can be equipped for SThM purpose with various thermo-sensors. These can be submitted to the different characteristic working modes:

(a) With exception of the mechanical sensor, the electrical sensorsones, in particular the thermocouple tip, allow to run the sensor in an unipolar or

Table 3
Proposed classification of Scanning Thermal Microscopes (SThM)

Instrument based on					
Thermal sensing		AFM		STM	
		Unipolar	Bipolar	Unipolar	Bipolar
Electrical	Thermocouple	+	+	+	+
	Resistance	(×)	+	(×)	(×)
	P-n junction	(×)	(×)	+	(×)
Mechanical Bimetal	–	–	+	–	(×)
Heating mode:	Sample or thermo-sensor				
Feed-back mode:	Active or passive				

+: realized and reported in literature.
(×): not yet reported in literature but possible.

a bipolar mode. Bipolar means, referring to Fig. 3, the two dissimilar conductors 1 and 2 (or the two electrical wires in Fig. 3(a)/(b)) form the thermocouple (or electrical resistance). The temperature sensing element constitutes a sample-independent detector with intrinsic sensitivity. It is fully separated from the surface studied, whereas in a so-called unipolar arrangement, the sample on one side and the tip on the other side commonly form the thermocouple junction or resistance, respectively.

(b) The temperature difference required for any thermal experiment results from heating either the probe or the sample. The heat is supplied either optically by a laser beam or resistively (by Joule heating). Uni- or bipolar mode can be combined with both heating modes.

(c) The selection whether the temperature signal controls the servo-loop or not introduces a further discrimination of the working modes: active or passive. In the passive mode, the probe operates without being heated and its temperature is monitored directly by one of the sensors described above, as it scans the sample surface. In the active mode, heater power is supplied always to the probe (tip) either by a current passing through the resistive sensor or from laser light shining on the tip. In both cases, the thermal conductivity of the sample influences the heat flow between probe and specimen. The active mode is implimented as constant-temperature mode. The heat flux from the probe to the sample (or inverse when the sample is heated) is held constant by changing as necessary the relevant feed back parameter, i.e. to keep a constant resistance for a resistive probe by either varying the current through the resistance or the distance between sample and probe, to keep a constant thermoelectric voltage or constant deformation of the bimetal by varying the distance between sample and probe.

It remains presently a fascinating and still open question for basic research to find out by which near-field process(es) the temperature information or heat, respectively, is transmitted within the short gap distance between the sample and the probe without mechanical contact. The various heat transport processes possible and considered are listed in Table 1 together with the theoretically expected distance dependence and the estimated power transferred. As far as we know none of the experiments reported in the literature could confirm one of the proposed gap-distance dependencies.

Finally, the individually chosen experimental working conditions open further possibilities for the various combinations of methods and working-modes described, e.g. experiments in vacuum, in reduced pressure of special gases or in air, experiments in which the tip touches the sample surface or contactless (tip-to-sample) measurements. The description given illustrates the broad scope of possible SThM arrangements. By far, not all the possible combinations have been probed. However, it becomes obvious that, in future, a clear notation of the dedicated instrumental set-up and its working conditions is desirable. Method, type of sensor and its working-mode, heating mode and type of servo-loop should be specified.

3.3. Scanning thermal microscopy-historical and experiments

The invention of the STM and AFM lead to a steady increasing number of STM/AFM equipment and sensors for the detection of various physical properties with sub-μm or better spacial resolution. Table 4 visualizes the historical development and lists the basic reports that had led to technological progress in this field. The table indicates the reference, the method used, the physical parameter measured and the resolution achieved. In the beginning, progress focused on developing and extending the STM/AFM technology, whereas in the last thee years interest centered on the elaboration of more sensitive and (with respect to temperature) locally better resolving thermo-tips. Table 5 summarizes a number of thermosensors recently reported in the literature. In the following we give a short description of the instrumentation and sensors referred to in Tables 4 and 5. At present, no comprehensive review is available, however, the essentials are contained in detail in the papers referenced in these two tables.

The first scanning thermal sensor was described by Williams and Wickramasinghe [41,42] and consisted of a thin-film rigid thermocouple at the end of a conventional STM tip (bipolar arrangement). The probe was heated and brought into proximity of the

Table 4
Historical development and various arrangements reported in the literature and performed experiments to measure various physical and chemical parameters. (dx, dV, dT, dt denote local, voltage, temperature and temporal resolution, respectively)

Ref.	Method	Measured quantity	Resolution reported
[41]	Tunneling microscope (bipolar)	Topography	dx ca. 50 nm
	- Thermocouple with heater	–	–
	- Feedback-loop with dT=0	–	–
[64]	Tunneling-Thermometer (unipolar)	Optical absorption	dx ca. 1 nm; dV/dt=4 μV/K
	- Thermocouple formed with sample	–	dVdT ca. 4 mV/K
	- Thermocouple heated with laser	–	–
[58]	same as ref. [54]	Chemical potential	dx ca. 5 nm
[62]	Atomic force microscope (unipolar)	Contact-potentials	dx ca. 10 nm
	- Thermocouple formed with sample	(W/SiO_2 vs. Pt/Si)	–
	- Heated tip	–	–
[63]	same as ref. [56]	Heat conductivity	dx ca. 200–500 nm; dV/dT ca. 3,5 μV/K
	- Heat loss by air from sample surface	(SiO_2 on Si)	–
[24,25]	AFM (bipolar)	Simultaneous	dx ca. 200 nm
	- Thermocouple	Topography/Thermography	dT ca. 0.1 K
[47,66]	AFM	Absorption and Heat of reaction	dE<10 pJ; dT=10^{-5}; dt ca. 3 μs
	- Micromechanical sensor	–	–
	- Bimetallic cantilever	–	–
[55,23]	AFM (bipolar)	Simultaneous	dx<1 μm; dt ca. 30 μs
	- Wollastone wire	Topography/Thermography	–
	- Thermometer is heater	–	–
[49]	AFM (bipolar)	Simultaneous	dx=400 nm; 360 mV/K
	- Bimetal (Al oder Au)	Topography/Thermography	–
[65]	AFM (bipolar)	Surface potentials	dx=200 nm
	- pn-junction	on Si pn junctions	dx=200 nm
[57,58]	AFM/STM (bipolar)	Thermography	dx=200 nm
	- Thermocouple sensor	–	–
	- Thermocouple with heater	–	–
[26]	STM (bipolar)	Heat conductivity	dx ca. 100 nm; dV/dT ca. 8 μV/K
	- Without heating thermocouple	Topography and Thermography	dT ca. 0.01 K, dt=50 ns
	- Measurement of absolute temperature	–	–
[46]	AFM	Simultaneous	–
	- Resistive heated sensor (Pt)	Topography/Thermography	–

surface. Using the temperature sensed by the thermotip as a feedback signal, to maintain a constant tip-to-specimen gap, this 'scanning thermal profiler' imaged topographically the surface of insulating samples [3,41,42,58,64]. Thus, this technique originated from the idea to scan insulating surfaces where the STM, at that time, was unable to do. In principle this problem was solved by the invention of the AFM, but it took some time to modify (and extend) the AFM technique to perform also the type of studies which are typical for STM: electron transport, contact potential, spectroscopy, etc. Williams and Wickramasinghe [3,41,42] obtained spatial resolution below 100 nm during thermal imaging and photothermal experiments. Weaver et al. [64] modified a STM tip to make a tunneling thermometer and measured optical absorption of thin metallic films with 1 nm spatial resolution. In this arrangement, the sample and the (STM) tip, made from different electrically conducting materials form the thermocouple junctions (unipolar arrangement) in order to monitor temperature differences on the sample surface. This technique measures the electron temperature based on the thermoelectric effect due to tunneling which leads to a measurable voltage difference. The authors reproduced the absorption spectrum of a thin gold film by changing the frequency of an incident laser beam that heated the gold film. Williams and Wickramasinghe [58] determined, with

the same arrangement as described in Ref. [64], electrochemical potentials with atomic scale resolution. The use of AFM for thermal imaging has a short history. Nonnenmacher et al. [62] studied the contact potential between a W-coated Si/SiO_2 substrate ad a Pt coated Si tip of an AFM. Later Kikukawa et al. [65] measured the surface potential of Si pn junctions with a Kelvin probe AFM. Nonnenmacher and Wickramasinghe [63] mapped the thermal conductivity of SiO_2 in the sub-μm scale. The technique is based on the temperature dependence of the contact potential between two metals and served to measure the variations of thermal conductivity of the samples studied. Barnes et al. [66,67] described a highly sensitive calorimeter based on the deflection of a bimetallic micromechanical sensor in conjunction with an AFM. The achieved energetical resolution ranges on the pW to fW scale. Scanning thermal imaging, performed simultaneously with atomic scale topography, the next naturally expected step in the evolution of thermal mapping, was reported recently by Majumdar and coworkers in several contributions [24,25,27]. It was demonstrated that thermo-sensors on a AFM cantilever enable one to measure temperature and thermal properties of any material. The authors fashioned an AFM cantilever with two wires which form a thermocouple junction as scanning tip to obtain simultaneously thermal and topographical images with submicrometer thermal resolution. The thermo-probe consists of two dissimilar wires, joined together to form a thermocouple as schematized in Fig. 3(b). The wire provides the cantilever spring constant and the thermocouple junction was electrochemically etched to provide a sharp tip. Dinwiddie et al. [23], Pylkki et al. [55], and Hammiche et al. [46] introduced another type of thermal probe, the resistance thermometer, and for that purpose adopted a Wollastone wire to an AFM cantilever which is used as heater and thermometer. Nakabeppu et al. [49] measured surface temperature differences by detecting the differential thermal expansion of a composite cantilever. Forster and Gmelin [26] determined the thermal conductivity (or diffusivity) and thermal boundary resistance at low temperatures with high spatial and temporal resolution using Pt or W vs. Au-0.07% Au thermotips, as described above.

4. Thermo-sensors

Thermocouple junction, resistive thermometers and bimetallic sensors are well-suited for nanofabrication. Therefore, as soon as the methodical capabilities of SThM based on AFM had been demonstrated, emphasis was given to the refinement and increase of sensitivity to produce better tip-sensors. Table 5 gives a survey and displays the state of the art of thermomicrosensors. The list indicates the characteristic features of the sensors as construction principle, materials used, tip radius, spatial, thermometric and temporal resolution. Some of the earlier thermocouple sensors were outlined before in the context of the

Table 5
Characteristic properties and performance of some of the micro-thermosensors described in the literature

Year	Ref.	Sensor material	Tip-radius r (μm)	Spatial resolution dx (μm)	Temperature–voltage–sensitivity V (μV/K)	Temporal Resolution t (ms)
86	[41,43]	?	0.1	<0.1	–	–
93	[54]	Chromel/Alumel	25	0.5	–	–
94	[23]	Pt wire-resistance	4	<1	[0.004 Ω/ΩK]	0.01–0.03
94	[47,48]	Al/SiN_x bimetal	–	–	[1 pJ; 10^5 K]	–
95	[26]	AuFe/W, Pt/Ir	0.1	0.2	0.5–12	0.05
95	[24,25]	Au/Pt auf Si_3N_4	0.01–0.03	0.5	8.6	–
95	[49]	Al/Si_3N_4	–	0.4	360 000	–
95	[45,56,57]	Au/Constantan	0.1	0.3–1	43	–
96	[40]	Si/Metal	0.5	<1	>300	<0.001
96	[69]	Au/Pt	0.1 $(100\ nm)^2$	0.075	5–6	–
96	[70]	NiCr/SiN	<1	–	8.4	–
96	[21]	Si-Thermopile	2000 (2×2 mm)	1–4	(0.02 K)	<1000

historical. In the following we discuss exclusively bipolar sensors that are mostly used. Only a few papers refer to unipolar tip arrangements (see e.g. Refs. [61,68]).

The prototype of thermal probe, reported in 1986 by Williams and Wickramsinghe [41,42] consisted of a conical tip with a thermocouple at its end. No further indications was given in view of the metal used. The resolution was better than 100 nm laterally and 3 nm vertically. Initially this sensor was used for topographical imaging (not for thermal). Then it proved as a powerful tool and was applied for various SThM experiments to study different physical properties as described in the previous section [33,41,42,58,61–64].

In 1993, Majumdar et al. [24] introduced another combination of materials for the fabrication of a thermocouple tip: Chromel vs. Alumel replaces the commercial AFM tip. This thermo-tip has a working junction of about 25 μm diameter in conjunction with a cantilever spring constant of 0.1–1 N/m. The spatial resolution for thermal profiles amounted to 0.5 μm (see Table 5).

In 1995, Forster and Gmelin [26] as well as Stopka [57] (and equally described in Refs. [56,57]) produced further thermo-tips based on the thermocouple-junction principle. Ref. [26] describes a low temperature wide-range (2–300 K) sensor made of Pt/Ir or W as usually applied in a STM. This miniature thermocouple is processed as follows, first, it is covered with insulation (thickness about 0.05 mm) in a way that a small distance (few μm) at the top end, and a small part (1–2 mm) at the rear end, remain free; then to form the thermocouple, a metallic film with a thickness, varying from one tip to the next, in the range of 50 nm is sputtered on the tip-surface, so that it covers the top [26]. The two metals at the rear end are in contact with 0.07 mm copper wires. These contacts must strictly be of the same temperature in order to ensure that the thermoelectric voltage, generated from the tip, is only dependent on the thermopower of the two metals joined. The authors selected Au-0.07% Fe as alloy for conductor 2 (see Fig. 3(a)) since that Kondo alloy generates an anomalous high thermopower at low temperatures. The Au-Fe coating was produced by use of an Au-0.07 Fe sputter target. During the sputter process, the tip is inclined by 30° and rotated to yield a homogeneous composition of the junction. The thermopower amounts to 8–12 μV/K and is displayed in Fig. 4(a). The sensor constructed by Stopka [57] consists of thin constantan wire (diameter 250 μm) at which at one end a tip, with a radius of about 100 nm, was etched electrochemically. Then epoxy resin covers the tip for electrical insulation before covering the resin with a 100–150 nm gold layer. The thermovoltage achieved is 43 μV/K near room temperature.

Majumdar et al. [25] discussed two other constructions. First, a small single crystal of diamond is stuck using epoxy to the end of the thermocouple referenced in Ref. [24], to provide a harder tip for higher spatial resolution. Second, a Si_3N_4 cantilever probe contains a sharp pyramid-shaped stylus that is 5 μ at the base and has a tip radius of 10–30 nm. The tip-legs, forming the thermocouple, are made of 350 Å thick gold and platinum films deposited on a SiO_2 film fit on the cantilever. The metal film overlap and thus form the thermocouple with an area of about $40\times40\ \mu m^2$. The sensitivity measured amounts to 8.6 μV/K. Nakabeppu et al. [49] describe a similar thermo-sensor.

Luo et al. [69] and Suzuki [70] report on novel thermo-probes designed and fabricated by using nanotechnology. A thin metal or conducting film is deposited on an about 500 nm thick SiN_x or Si cantilever, e.g. 500 nm Ti/Au (Ti as buffer layer). In order to form the thermo-junction (tip), a 1000 Å layer of SiO_2 is deposited on which the buffer of Ti (50 Å) and the thermoelectric material Au (380 Å) films are evaporated. A nanohole, as the essential feature of this construction, is then made in the Pt-film when it is brought in contact with a conducting sample, using the AFM. A voltage pulse, applied to the tip and sample and due to the high electric field localized around the tip, evaporates the thin film and opens a hole only at the very end of the tip. This hole diameter created is around 100 nm (3 V during 10 ms for a 500 Å film). The sensitivity measured is 6 μV/K near room temperature. Suzuki [70] fabricated an integral pyramidal thin-film micro-thermocouple. The two dissimilar metallic thin films which form the thermocouple are deposited on a free-standing SiN_x microcantilever (lengths from 180–880 μm). A pyramidal Si-micropit was etched lithographically onto the end of the cantilever and then covered by SiO_2. A layer of 100 nm of NiCr and 50 nm Ti were created by electron beam evaporation and thus form the thermo-junction. The lithographical fabrication of this thermo-tip is quite

elaborated and the reader is referred to Ref. [61] for further details. The thermoelectric sensitivity was measured to be 8.4 μV/K.

Recently, Fischer et al. [40] demonstrated the feasibility of high resolution thermo-tips over a large temperature range from 4–300 K which is described here for the first time. This miniature thermocouple consists of a doped semiconductor (Si with $n \approx 10^{19}$ cm^{-3}) needle with dimensions similar to conventional STM-tips (diameter about 0.25 mm, length about 5 mm). The needle is covered with insulation (SiO_2, thickness about 100 nm) such that, like described earlier [26], a few μm at the tip-apex and about 1 mm at the rear end remain free. Then, to form the thermocouple, a thin (ca. 200 nm) Au-film is evaporated on the tip surface covering the top but remaining free both the rear part as well as a small portion (ca. 1 mm) of the insulation. Finally, again similarly as described in Ref. [26], the Au-film and the rear end of the semiconductor needle are contacted with copper wires allowing to monitor the thermoelectric voltage generated from the thermocouple junction at the tip-apex. The Seebeck coefficient of this microthermocouple (see Fig. 4(b)) reaches values of >300 μV/K, probably the best values reported up till now. The thermal response time of this sensor is shown in Fig. 4(b) and is below 10 μs.

In the class of resistive thermo-sensors, Pylkki et al. [61] and Dinwiddie et al. [23] introduced the first probes which were used both as thermometer and heater. Currently these probes are fashioned from Wollastone wire which consists of the core, typically platinum with a diameter of ca. 5 μm, surrounded by a thick silver coating of about 75 μm thickness. A loop of the Wollastone wire is formed and attached to the cantilever of the AFM and forms the arms (length about 4 mm) of the cantilever as shown in Fig. 3(a). The silver coating is etched and uncovers a small thermal sensing length of the Pt-wire, approximately 200 μm long. The sensitivity (of the Pt-wire corresponds to the thermal resolution of usual platinum resistance thermometers and has a spatial and temporal resolution of about 1 μm and 10–30 μs, respectively (see Table 5).

With respect to bimetal as sensor, there exists a basic difference in application in an AFM. These sensors have been used always as sample support, i.e. the heat generated by a thermoanalytical process is detected (and not only the temperature) whereas in the types of sensors afore-mentioned, the temperature of samples, not being located on the measuring device (cantilever or tunneling), have been monitored.

Gimzewski et al. [47] fabricated one of the first micromechanical probes, as schematized in Fig. 3(c), a micromechanical Si cantilever (length 400 μm, width 35 μm and thickness 1.5 μm) coated with a thick layer (0.4 μm) of Al which both, Si and Al, form the bimetallic sensor. The sample to be studied is mounted upon this bimetal device. In fact the sensor is a heat-flux measuring device that induces a deflection of the bimetallic sensor due to the differential thermal expansion (see also Fig. 2). The device displays a very high temperature and heat (energetical) resolution of 0.01 mK and some nJ, respectively and very short relaxation times of less than 3 ms. In a later paper, Berger et al. [48] from the same group, describe a modified, fast and extremely sensitive cantilever system: It consists of a 'V'-shaped SiN_x cantilever with a 50 nm gold layer as micromechanical sensor in the form of a bimetallic strip [65]. With the same type of sensors Barnes et al. [66,67] resolved 150 fJ in photothermal experiments. Such bimetallic cantilever-sensors served also for the determination of the influence of vapors on surface stress [51–53]. Nakabeppu et al. [49] presented a composite cantilever probe similarly constructed as the bimetals described before. Al or Au was evaporated on the SiN_x cantilever. The temperature and spatial resolution were reported as being 0.1 K and 0.4 μm, respectively.

Fabrication of chip sensors, e.g. thermopiles on a mm-sized chip, for thermo-analytical instrumentation (calorimetry, reaction kinetics) is field that is rapidly growing. Although being of great practical interest, because it is expected that this technique soon enters the state of commercialization, it should not be discussed here; for some details see e.g. Ref. [21] and contributions in this volume.

Although the junction size in general is in the order of 10 μm, we note that the spatial resolution achieved in thermal mapping is found to be 10–20 times higher, i.e. 500 nm. This is presumably due to near field heat conduction effects between tip and sample. Scaling down the size of the thermocouple junctions will equally shorten the thermal response time of the tip-sensors from ms to the 10–100 ns range.

The calibration of the thermosensors is important and critical. To calibrate, usually the indication from a standard type thermocouple or calibrated Peltier-cooler/heater is brought into contact with the sample surface studied by the STM or AFM techniques.

5. Thermal imaging, applications and limitations

Simultaneous topographical and thermographical mapping on nanometer scale presumably is the most interesting feature of the SThM. In that view, the AFM technique has become the preferred experimental tool since it is most suitable for the majority of applications. The tip-to-surface force is used as feedback independent of the type of thermo-sensor applied, the surface property of the sample and the physical property studied. STM technique, however, has limited use, e.g. electrically non-conducting and biased electronic devices materials are excluded from the investigation. We note:

- Thermal imaging with simultaneous topography of the sample surface is on the way to become a routine technique, entering the state of commercialization. AFM technique is the preferred and most advantageous construction for that purpose (see Table 5 for refs.).
- The earlier experiments in this field, besides the topographical studies, prepared the basis for

- any type of sub-μm thermometry, useful for studies of thin films, interface and multi layers, compound materials,

- nanometer scale photothermal spectroscopy and microscopy,

- local measurement of coefficient of diffusivity, of heat capacity, contact potential, etc.,

- in situ temperature profiling of electronic and micromechanical devices (under load),

- detection of heat release in chemical and physical (e.g. photothermal) reaction in the pico- and femto-Watt scale or below,

- thermal analysis in the pico-liter range with solids or liquids or in the solid–liquid–gas system,

- the study of single atom or molecular reaction kinetics,

- sub-surface imaging, e.g. of inclusions of metals in polymers.

SThM technology provides the best spatial resolution among the existing thermometric methods to map microstructures, in particular semiconductor devices. The technique has the advantage that any modification of the sample investigated is not necessary.

There is one particular advantage of the SThM micro technique with respect to thermal analysis: The enormously reduced mass of the probing thermometer, with response times far below micro-seconds, enables for the first time the study of chemical reactions with thermometers which are quicker than the process studied itself. Most of the earlier-described thermoanalytical instrumentation displays instrumental-intrinsic thermal relaxation times in the sec-range whereas now the micro-sec ranges are explored also.

However, the method has some serious drawbacks and also bears the risque of performing useless experiments:

- the temperature drop between the scanning tip and the sample-surface is difficult to determine quantitatively,
- the tip-to-surface thermal conductance is influenced by topographical features which may vary the tip-to-surface temperature drop during a scan and vice versa,
- the variation of the sample thermal conductivity on the microstructural scale also modifies the temperature drop tip-to-surface,
- the arrangement is considerably sensitive to higher frequency electrical, capacitive and voltage-reflectance effects, particularly on the short-time scale experiment (>10 kHz).

Therefore, the scientist or engineer working with SThM's must be aware of the limitations given by the 'macroscopic' physical laws. In particular, Boltzmann's equation describes the transport phenomena – the heat transfer involved in all SThM experiments – only within certain limits. That requires re-definition of some of the physical parameters in the micro- or nanometer scale. For instance, calorimetry, chemical reaction-study and other thermo-analytical measurements already become questionable in the micrometer/nano-liter scale since the influence of surface effects, surface-energy, thermal equilibrium, a.o. effects may perturbate the results in comparison to the classical description. Such experiments therefore don't allow extrapolation of the gained data to large

masses or volumes. In addition, the calibration of absolute temperature, and even sometimes of the relative temperature changes are difficult or impossible. As a consequence, thermo-physical/chemical measurement require careful testing to find out and detect the limits of validity of the parameters involved, under the given conditions of reduced dimensionality, i.e. inspection of the mass or volume dependence, dependencies on scanning speed (upon the surface), thermal relaxation time of probe or/and sample, sample thickness, influence of surface size, etc., as it required for instance for scanning calorimetry [71].

6. Conclusion

Less than one decade after the invention of the scanning tunneling and atomic force microscope, this event caused, within a few years, a revolution in the instrumentation for measuring thermo-physical and thermo-chemical properties of matter. It will become in future of fundamental importance for mesoscopic-scaled thermal experiments measurements. The scanning thermal microscopy (SThM), derived from STM/AFM technique has rapidly attracted an interest. The feasibility of simultaneous topography on the atomic scale and temperature imaging (thermography) in the sub-μm scale has been demonstrated as well as the detection of a variety of physico-chemical parameters, e.g. temperature profiles, heat conductivity heat capacity, heat of transition, contact potential, scanning, subsurface inclusions, etc. A multitude of instrumental arrangement for the SThM were reported recently, however, many other experimental arrangements are conceivable but have not been yet realized. The technological development of thermo-tips with higher sensitivity accelerated impressively in the last three years. Thermal studies in physics and chemistry on the mesoscopic and atomic scale are under way and mainly focus on localized nanometer-scale photothermal spectroscopy (and may provide in the near future molecular spectra) and thermal analysis, thermal imaging and sub-surface imaging, i.e. inclusions of materials different from that of the sample and investigation of solid–solid interfaces. Modulation techniques will improve most probably the thermal resolution by reduction of electrical noise. Nevertheless, there remains a number of fundamental problems to be solved by basic research to take full profit of this new technology: the impact of short-time Joule-heating, transient phenomena in the framework of the Boltzmann equation, handling of multiple Boltzmann equations (with moments for electrons and phonons) and electron–phonon interaction, near-field effects and its influence on the measured tip-temperature, etc. In future, for the design of micro-electronic devices, presumably the thermal design aspects will become more important than the electronic design features; equally, the thermal design of micro-mechanical devices and thermo-chemical micro-instrumentation will become important.

This contribution has surveyed the historical development and gives the present state of the art of the SThM. Also, a classification scheme for the various experimental arrangements is proposed. It may be fascinating to observe which new ideas and applications will emerge in future from this relatively young field. Its high validity for basic and applied research is already today unquestionable.

References

[1] G. Binnig, H. Rohrer, Ch. Gerber, E. Weibel, Phys. Rev. Lett. 49 (1982) 57; G. Binnig, C.F Quate, Ch. Gerber, Phys. Rev. Lett. 56 (1986) 930.
[2] D. Sarid, Scanning Force Microscopy, Oxford University Press, New York, 1991; Sci. Am. 260 (1989) 98.
[3] C.C. Williams, H.K. Wickramasinghe, Appl. Phys. Lett. 49 (1986) 1387.
[4] D. Mate, D. McClelland, R. Erlandsson, S. Chiang, Phys. Rev. Lett. 59 (1987) 1942.
[5] Y. Martin, H.K. Wickramasinghe, Appl. Phys. Lett. 50 (1987) 11455.
[6] Y. Martin, D.W. Abraham, H.K. Wickramasinghe, Appl. Phys. Lett. 52 (1988) 1103.
[7] C.D. Bugg, P.J. King, J. Phys. E. Sci. Instrum. 21 (1988) 147.
[8] M.J. Kelly, in: M.J. Kelly, C. Weisbuch (Eds.), The Physics and Fabrication of Microstructure and Microdevices, Springer, Heidelberg, 1986, pp. 174–196.
[9] K.E. Goodsen, Y.S. Yu, M. Ashegi, Thermal Phenomena in Semiconductor Devices and Interconnects, in: C.L. Tien, A. Majumdar, F. Gerner (Eds.), Microscale Energy Transport, Taylor and Francis, Washington DC, 1997.
[10] S.M. Sze, VLSI Technology, Mc Graw Hill, 2nd ed., New York, 1988.
[11] R. Trcinski, E. Gmelin, H.J. Queisser, Phys. Rev. B 35 (1987) 6373.
[12] R. Trcinski, E. Gmelin, H.J. Queisser, Phys. Rev. Lett. 56 (1986) 1086.

[13] U. Gerlach-Meyer, H.J. Queisser, Phys. Rev. Lett. 51 (1983) 1904; U. Gerlach-Meyer, Appl. Phys. A 33 (1984) 161.
[14] L. Weber, E. Gmelin, H.J. Queisser, Phys. Rev. B 40 (1989) 1244.
[15] K.E. Goodson, M.I. Flik, ASME HTD 253 (1993) 23.
[16] L. Weber, M. Lehr, E. Gmelin, Phys. Rev. B 46 (1992) 9511.
[17] Le Hang Nguyen, H. Riegel, M. Asen-Palmer, E. Gmelin, Physica 218 (1996) 248.
[18] R. Dingle, Confined Carrier Quantum States in Ultrathin Semiconductor Heterostructures. Festkörperprobleme XV, H.J. Queisser (Ed.), Springer, Berlin, 1975, pp. 21–48.
[19] K. von Klitzing, G. Dorda, M. Pepper, Phys. Rev. Lett. 45 (1980) 484.
[20] M.B. Callan, Thermodynamics and An Introduction to Thermostatics, Wiley-Interscience, 2nd ed., New York, Chap. 4, 1985.
[21] J. Lerchner, J. Seidel, G. Wolf, E. Weber, Sensors and Actuators B 32 (1996) 71; J. Lerchner, R. Oehmgen, G. Wolf, P. LeParlout, J.-L. Daudon, High Temperatures–High Pressures, in press.
[22] H. Fiehn, T. Wegener, S. Howitz, Bioforum, 1–2 (1997); S. Fischer-Frühholz, BioTec. 1 and 4 (1997).
[23] R.B. Dinwiddie, R.J. Pylkki, P.E. West, Thermal Conductivity 22 (1994) 668.
[24] A. Majumdar, J.P. Carrejo, J. Lai, Appl. Phys. Lett. 62 (1993) 250.
[25] A. Majumdar, J. Lai, M. Chandrachood, O. Nakabeppu, Y. Wu, Z. Shi, Rev. Sci. Instrum. 66 (1995) 3584.
[26] R. Forster, E. Gmelin, Rev. Sci. Instrum. 67 (1996) 4246.
[27] A. Majumdar, Exp. Heat Transfer 9 (1996) 83.
[28] E. Doebelin, Measurement Systems: Application and Design, McGraw-Hill, 3rd ed., New York, 1985; L.C. Rubin, B.L. Brandt, H.H. Sample, Cryogenics 22 (1981) 491.
[29] J.W. Valvano, Advances in Heat Transfer 22 (1992) 359.
[30] R.L. Powel, W.J. Hall, C.H. Hyink, L.L. Spaks, G.W. Burns, M.G. Scrogen, H.H. Plumb, Thermocouple Reference Tables based on IPTS-68 NBS Monograph 125, U.S. Governm. Publ. Office, Washington DC, 1974.
[31] T.Q. Qiu, C.P. Grigopoulos, C.L. Tien, Experimental Heat Transfer 6 (1993) 23.
[32] R. Ostermeir, K. Brunner, G. Abstreiter, W. Weber, ASME, J. Electron. Packaging 113 (1991) 286.
[33] D.L. Barton, P. Tanyunyong, Microelectronic Engineering 31 (1996) 271.
[34] Y. Martin, H.K. Wickramasinghe, Appl. Phys. Lett. 50 (1987) 168; W. Claeys, S. Dilhaire, V. Quintard, J.P. Dom, Y. Danto, Reliability Engineering International 9 (1993) 303.
[35] A. Mandelis, Photoacoustic and thermal wave phenomena in semiconductors, North Holland, New York, 1989.
[36] A. Mandelis, Progress in Photothermal and Photoacoustic Science and Technology, Elsevier, New York, 1992.
[37] K.E. Goodsen, M. Asheghi, Microscale Thermophysical Engineering, preprint and references therein.
[38] Y.S. Yu, O.W. Käding, Y.K. Leung, S.S. Wong, K.E. Goodsen, IEEE Electro Device Letters 18 (1997) 169.
[39] Y. Sungtaek, K.E. Goodsen, Proc. 35th IEEE Int. Reliability Physics Symp., IEEE Catalog No. 97CH35983.
[40] R. Fischer, private communication.
[41] C.C. Williams, H.K. Wickramasinghe, in: P. Hess, J. Peizl (Eds.), Photoacoustic and Photothermal Phenomena, Springer Series on Optical Sciences, Springer, New York, 1988, p. 364.
[42] C.C. Williams, H.K. Wickramasinghe, Proc. SPIE 897 (1988) 129.
[43] K. Dransfeld, J. Xu, J. Microsc. 152 (1988) 35.
[44] R. Möller, C. Baur, A. Esslinger, J. Kirz, J. Vac. Sci. Technol. B 9 (1991) 609.
[45] E. Oesterschulze, M. Stopka, L. Ackermann, W. Scholz, S. Werner, J. Vac. Sci. Technol. B 14 (1996) 832.
[46] A. Hammiche, D.J. Hourston, H.M. Pollak, M. Ready, M. Sous, J. Vac. Sci. Technol. B 14 (1996) 1486.
[47] J.K. Gimzewski, Ch. Gerber, E. Meyer, R.R. Schlittler, Chem. Phys. Lett. 217 (1994) 589.
[48] R. Berger, Ch. Gerber, J.K. Gimzewski, E. Meyer, H.J. Güntherodt, Appl. Phys. Lett. 69 (1996) 40.
[49] O. Nakabeppu, M. Chandrachood, Y. Wu, J. Lai, A. Majumdar, Appl. Phys. Lett. 66 (1995) 694.
[50] E. Meyer, J.K. Gimzewski, Ch. Gerber, R.R. Schlittler, in: M.E. Welland, J.K. Gimzewski (Eds.), The Ultimate Limits of Fabrication and Measurement, Kluwer, Dordrecht, The Netherlands, 1995, p. 85.
[51] T. Tundar, R.J. Warmarck, G.J. Chen, D.P. Allison, Appl. Phys. Lett. 64 (1994) 2894.
[52] T. Tundar, E.A. Wachter, S.L. Sharp, R.J. Warmick, Appl. Phys. Lett. 66 (1995) 1695.
[53] V. Foglietti, M.P.C. Kuijper, S. Petrocco, P. Russo, A. Bearzotti, in: G. Padeletti, A. d'Amico (Eds.), Proc. of 1st Italian Conf. on Sensors and Microsystems, World Scientific, Singapore, 1996, pp. 351–355.
[54] K. Fushinobu, A. Majumdar, K. Hijikata, ASME J. Heat Transfer 117 (1995) 25.
[55] R.J. Pylkki, P.J. Moyer, P.E. West, Jpn. J. Appl. Phys. Part 1 33 (1994) 3785.
[56] E. Oesterschulze, R. Kassing, J. Vac. Sci. Technol. B 13 (1995) 2153.
[57] M. Stopka, E. Oesterschulze, J. Schulbe, R. Kassing, Mater. Sci. Eng. B24 (1994) 226.
[58] C.C. Williams, H.K. Wickramasinghe, Nature 344 (1990) 317.
[59] P. Muralt, D.W. Pohl, Appl. Phys. Lett. 48 (1986) 514.
[60] P. Muralt, K. Meier, D.W. Pohl, H.W.M. Salemik, Appl. Phys. Lett. 50 (1987) 1352.
[61] R.C. Davis, C.C. Williams, P. Nasil, Appl. Phys. Lett. 66 (1995) 2309.
[62] M. Nonnenmacher, M.P. Boyle, H.K. Wickramasinghe, Appl. Phys. Lett. 58 (1991) 2921.
[63] M. Nonnenmacher, M.K. Wickramasinghe, Appl. Phys. Lett. 61 (1992) 168.
[64] J.M. Weaver, L.M. Walpita, H.K. Wickramasinghe, Nature 342 (1989) 783.
[65] A. Kikukawa, S. Hosaka, R. Imura, Appl. Phys. Lett. 66 (1995) 3510.
[66] J.R. Barnes, R.J. Stephenson, C.N. Woodburn, S.J. O'Shea, M.E. Welland, T. Rayment, J.v. Gimzewski, Ch. Seitzer, Rev. Sci. Instrum. 65 (1994) 3793.

[67] J.R. Barnes, R.J. Stephenson, M.E. Welland, Ch. Geher, J.K. Gimzewski, Nature 372 (1994) 79.
[68] A. Rettenberg, C. Baur, K. Länger, D. Hoffmann, J.Y. Grand, R. Möller, Appl. Phys. Lett. 67 (1995) 1217.
[69] K. Luo, Z. Shi, J. Lai, A Magundar, Appl. Phys. Lett. 68 (1996) 325.
[70] Y. Suzuki, Jpn. J. Appl. Phys. 35 (1996) L352.
[71] E. Gmelin, St.M. Sarge, J. Appl. Chem. 67 (1995) 1789.